arXiv:cond-mat/0308512v2 [cond-mat.supr-con] 29 Aug 2003

Dynamic ordering and frustration of confined vortex rows studied by mode-locking experiments

N. Kokubo, R. Besseling and P. H. Kes
Kamerlingh Onnes Laboratory, Leiden University,P.O.Box 9504, 2300 RA Leiden, The Netherlands
(February 2, 2008)

The flow properties of confined vortex matter driven through disordered mesoscopic channels are investigated by mode locking (ML) experiments. The observed ML effects allow to trace the evolution of both the structure and the number of confined rows and their match to the channel width as function of magnetic field. From a detailed analysis of the ML behavior for the case of 3-rows we obtain (*i*) the pinning frequency f_p, (*ii*) the onset frequency f_c for ML ($\propto$ ordering velocity) and (*iii*) the fraction L_{ML}/L of coherently moving 3-row regions in the channel. The field dependence of these quantities shows that, at matching, where L_{ML} is maximum, the pinning strength is small and the ordering velocity is low, while at mismatch, where L_{ML} is small, both the pinning force and the ordering velocity are enhanced. Further, we find that $f_c \propto f_p^2$, consistent with the dynamic ordering theory of Koshelev and Vinokur. The microscopic nature of the flow and the ordering phenomena will also be discussed.

I. INTRODUCTION

Vortex arrays (VA's) in type II superconductors are exemplary systems to study non-equilibrium states of driven periodic media in various pinning environments. A particularly interesting phenomenon in this context is that of a dynamic transition from an elastic, coherent flow state at large velocities to a plastic, incoherent flow state at small velocities. The first theoretical description of this issue was provided by Koshelev and Vinokur (KV) [1] and refined in subsequent studies [2–5] which predicted various novel flow states, including a moving glass characterized by elastically coupled chains oriented along the flow direction and a moving transverse smectic with decoupled flow chains. Such structures and the dynamic transitions between them have been extensively studied in a number of numerical simulations [5–7].

Experimentally, a diversity of flow states has been reported in direct imaging experiments on $NbSe_2$ crystals [8–10]. However, quantitatively the effect of pinning strength and/or temperature on the ordering velocity has been studied only through dc transport experiments [11–13], based on the assumption that an inflection point in dc current-voltage (IV) curve (i.e. a peak in differential resistance) marks the dynamic transition. Recently, different explanations have been given as the reason for such inflection point, like macroscopic coexistence of two phases [14] and a change in the self organized, large scale morphology of vortex rivers [15]. Thus, a more direct, microscopic probe is required to study systematically the velocity, magnetic field and temperature dependence of dynamic ordering.

Recently, we reported on the use of mode-locking (ML) experiments as a direct probe of ordering [16]. The ML phenomenon occurs due to coupling between, on the one hand, collective lattice modes of frequency $f_{int} = qv_{dc}/a$, with q an integer and a the lattice periodicity, which occur when a VA moves coherently with velocity v_{dc} through a pinning potential [10,17], and, on the other hand, a superimposed rf-drive of frequency f at an integer fraction $1/p$ of f_{int}. This coupling produces steps in the dc-transport (IV) curves when $v_{dc} = (p/q)fa$ [7,18–21], similar to ML steps in sliding charge density waves (CDW's) [22,23] and giant Shapiro steps in Josephson junction arrays [24]. However, on decreasing the velocity v_{dc} or increasing the temperature, incoherent velocity fluctuations due to quenched and thermal disorder suppress the collective lattice mode and reduce the width of the ML steps. Approaching the regime of fully plastic or liquid flow, the ML amplitude eventually vanishes [7,16] and the ML frequency f_c at which this occurs provides a *direct* measure of the ordering velocity: $v_c = f_c a$.

The particular system of our studies consists of mesoscopic flow channels in a disordered, strong pinning environment [21,25]. The geometry of the samples is sketched in Figs. 1(a),(b). Vortices inside the channels are confined by strongly pinned vortices in the channel edges (CE's). When a force is applied along the channel, the shear interaction with these CE vortices provides the dominant pinning mechanism impeding the channel flow. Further, since the natural lattice (row) spacing is $a_0 \simeq 1.075\sqrt{\Phi_0/B}$ ($b_0 = \sqrt{3}a_0/2$), on varying the magnetic field B one can go through a series of structural transitions from n to $n \pm 1$ vortex rows in the channel (typically $n \lesssim 10$). Besides its relevance for the study of (dynamic) structural transitions of vortex matter in quenched disorder, the physics of this system is also closely related to layering transitions in confined fluids, flow of colloids in mesopores and mesoscopic friction.

In Ref. [21] we have given a short account of the interesting phenomena which this system displays. Firstly, due to the structural transitions, the dc-critical current

for channel flow (yield strength) oscillates with field as shown in Fig. 1(e). At a given field, the dc IV (force-velocity) curve *with* superimposed rf-current exhibits the ML effect, as shown in Fig. 1(c). The ML condition in this case attains a form which is particularly useful to study the structural transitions. The voltage $V_{1,1}$ at which the fundamental($p = q = 1$) ML step occurs is given by [21]:

$$V_{1,1} = f\Phi_0 n N_{ch} \tag{1.1}$$

with Φ_0 the flux quantum, N_{ch} the number of channels measured simultaneously and n the *number of coherently moving chains* in each channel.

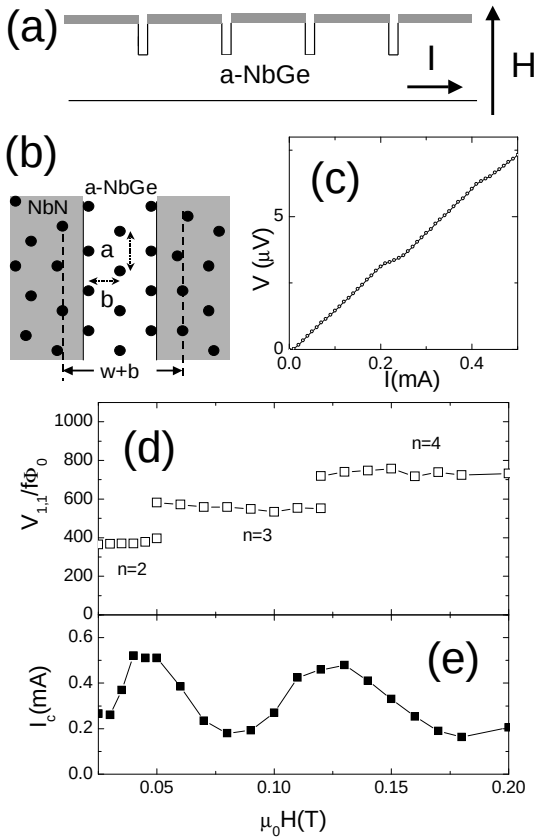

FIG. 1. (a) The channel device (side view) consisting of strong pinning NbN (dark) and weak pinning amorphous NbGe. The current and field directions are indicated. (b) Sketch of the vortex structure around a channel (top view). The effective channel width w is also indicated. (c) Typical ML step in a dc-IV curve at 70mT and a superimposed rf-current of 3MHz. (d) Normalized ML voltage $V_{1,1}/(f\Phi_0)$ versus magnetic field. (e) Critical current I_c, determined from a 1μV criterion, versus field.

As observed in Fig. 1(d), on changing field, $V_{1,1}$ increases as a staircase, directly reflecting the evolution of n with field . A comparison with Fig. 1(e) shows that at mismatch fields, i.e. where a transition $n \to n \pm 1$ occurs and n and $n \pm 1$ steps may coexist, the yield strength $\propto I_c$ is maximum, whereas around the center of the $V_{1,1}$ plateau, where an n row configuration matches the channel width, it is minimum. As shown in Ref. [21], this phenomenon is caused by positional disorder (roughness) of the vortex configuration in the CE's: first of all, on moving away from the matching field this disorder enhances transverse fluctuations of vortex chains in the array, impeding the flow. Secondly, close to mismatch, part of the (moving) n-chain regions within each channel may switch to $n \pm 1$. In between the n and $n \pm 1$ regions quasi-static fault zones with misaligned dislocations develop where the vortex trajectories are jammed. We note that the presence of degrees of freedom transverse to the average flow velocity, both in our system and vortex lattices in general, forms an important difference with CDW's. Particularly, for CDW's the 'displacement' (phase) field is a scalar $\phi(x)$ and the velocity $\propto \partial_t \phi(x)$ represents longitudinal motion only. Our system, when compared to regular vortex lattices, has the unique property that the transverse response can be tuned.

In this paper we study in detail the ML step width as function of the rf-amplitude and frequency. The experiments provide important information on the dynamic coherence of the arrays and how this coherency varies with mismatch and flow velocity. We focus on ML in the regime where $n = 2 \to 3 \to 4$, but our findings are representative for other transitions with limited $n \lesssim 10$. The paper is organized as follows. In Sec. II we first review previous theoretical results on ML at high frequency and then present simulation results of a one dimensional (1D) vortex chain to show the full frequency dependence of ML in a system with only elastic deformations. In Sec. III we describe the details of our sample and the experimental procedure. The experimental results are presented in Sec. IV. We find clear evidence for an *ordering* frequency f_c below which no ML occurs. Furthermore, from the ML data we extract the pinning frequency f_p and the total length L_{ML} of coherently moving 3-row regions. These quantities systematically change with magnetic field: at matching, where L_{ML} is large, f_p and f_c are both small, while at mismatch where L_{ML} is small, both f_p and f_c are enhanced. We find that $f_c \propto f_p^2$, independent of magnetic field. In Sec. V we compare these results with the ordering theory of Koshelev and Vinokur, and discuss the implications for the microscopic nature of the flow and the ordering phenomena.

II. THEORETICAL CONSIDERATIONS

The velocity (or frequency) dependence of the ML step width is particularly useful as a direct probe of dynamic ordering. At present, the ML step width has been studied theoretically only in the high frequency limit, where perturbation theory allows to obtain an analytical description [26–28].

A. Equation of motion

The 2D displacement field $\vec{u}(\mathbf{r},t)$ of an elastic vortex lattice driven through a pinning environment by combined rf and dc external forces is (at $T=0$):

$$\gamma\frac{\partial\vec{u}}{\partial t}=\mathbf{F_D}+\mathbf{F_R}+\mathbf{F_P} \tag{2.1}$$

with $\gamma=\Phi_0 B/\rho_f$ the friction coefficient with ρ_f the flux flow resistivity. $\mathbf{F_D}$ is a driving force per unit length consisting of dc and rf terms; $|\mathbf{F_D}|=j_{dc}\Phi_0+j_{rf}\Phi_0\cos(2\pi ft)$ with j_{dc} and j_{rf} the dc and rf current densities, respectively. $\mathbf{F_R}$ is the elastic restoring force given by $(\Phi_0/B)[(c_{11}-c_{66})\nabla(\nabla\cdot\vec{u})+c_{66}\nabla^2\vec{u}]$ with c_{11} and c_{66} the compression and shear moduli, respectively [1,5]. In absence of the pinning force $\mathbf{F_P}$, the lattice is undistorted and flows uniformly: $du/dt=\mathbf{F_D}/\gamma=v_{dc}+v_{ac}\cos(2\pi ft)$ with an ac velocity $v_{ac}=j_{rf}\Phi_0/\gamma$, i.e. proportional to the rf-drive.

B. Amplitude of the ML-interference step

At high velocities where the friction term dominates the pinning term in Eq.(2.1), one can treat the pinning as a perturbation with respect to the undisturbed rf-dc velocity $|\mathbf{F_D}|/\gamma$. We distinguish two cases, namely a periodic pinning potential and a random pinning potential. In case of a periodic potential with periodicities equal to that of the lattice, elastic deformations are absent ($\mathbf{F_R}$=0) and the whole lattice behaves as a single particle with overdamped dynamics in a sinusoidal potential. At large drive this case is described analogous to a voltage biased, resistively shunted Josephson junction [29]: substituting $u=vt$ in Eq.(2.1) and assuming $F_P=\mu\sin(ku)$ with μ the maximum slope of the potential and $k=2\pi/a$, one can show that as first order correction a step anomaly appears in the dc velocity-force characteristics at the ML condition $v_{dc}=paf$. The current density width of the pth step oscillates with the rf-drive according to

$$\Delta j_{p,1}=2j_c|J_p(v_{ac}/fa)| \tag{2.2}$$

with $j_c=\mu/\Phi_0$ the critical current density and J_p the Bessel function of the first kind of order p. Note that no subharmonic ML ($q\geq 2$) occurs in this model.

Turning to a VL in a purely random potential, the first order perturbation correction has zero mean. The second order correction is the lowest order of perturbation that provides the ML step. Taking into account the lattice distortions due to the random pinning within the elastic limit, Schmidt and Hauger [26] showed that the ML step can appear at both harmonic and subharmonic ML conditions $v_{dc}=(p/q)af$ and that the associated width of the current density step is:

$$\Delta j_{p,q}=2\tilde{j}_c(qk)J_p^2(qv_{ac}/fa) \tag{2.3}$$

$$j_c=\sum_q \tilde{j}_c(qk) \tag{2.4}$$

where $\tilde{j}_c(qk)$ is the component of the critical current density related to the Fourier transform of the random potential correlator at wave vector qk. Thus, for random pinning the ML step width exhibits a squared Bessel-function oscillation with the rf drive. In the following we omit the subscripts p and q in the ML step width since we will discuss only the fundamental ML phenomenon for $p=q=1$ (where $q=1$ will be justified in Sec. IV). We note here that in our case a can be a frustrated lattice spacing opposed to the natural one in [26].

C. Frequency dependence

It is clear in Eqs.(2.2) and (2.3) that the dependence on frequency and rf drive only appear in the argument $z=v_{ac}/fa$ of the Bessel functions, irrespective of the type of pinning. Choosing z by varying the rf-amplitude such that $J_1(z)$ is maximum, the characteristic maximum value of the fundamental ML width at high frequency is

$$\Delta j_{max,P}=1.16j_c \tag{2.5}$$

$$\Delta j_{max,R}=0.67\tilde{j}_c(k) \tag{2.6}$$

for periodic and random pinning, respectively.

These perturbational results are only applicable for frequencies (much) above the so-called pinning frequency f_p. For a sinusoidal pinning potential, f_p is analogous to the characteristic frequency of an overdamped Josephson junction and it is given by:

$$f_p\equiv j_c\Phi_0/\gamma a. \tag{2.7}$$

For random pinning, the fundamental ML step involves only the $k=2\pi/a$ Fourier component of the pinning force, $\tilde{F}_p(k)=\tilde{j}_c(k)\Phi_0$ since it is responsible for the dynamic lattice mode excited at the washboard frequency ($f_{int}=v_{dc}/a$). In this case one can define the pinning frequency f_p [30] such that the strength of the friction term γaf in Eq.(2.1) equals $\tilde{F}_p(k)$:

$$f_p\equiv\tilde{j}_c(k)\Phi_0/\gamma a. \tag{2.8}$$

Below f_p no analytical result for Δj_{max} is available, not even for sinusoidal pinning [31]. In this regime numerical simulations are a useful tool to obtain the theoretical value of the fundamental ML width [32,33]. To obtain Δj_{max} vs. f for the case of completely elastic motion in our channel system, we have performed molecular dynamics simulations of an rf-dc driven 1D *elastic* vortex chain both in a channel with periodically configured static vortices in the CE's and in channels with strongly disordered CE vortex arrangements (see the inset of Fig.

2(c) and [34,35] for more details). The channel width $w = b_0$, i.e. the (average) spacing between the first pinned rows is $2b_0$. Vortex interactions were modelled by the London potential with $\lambda/a_0 = 1$ (λ is the penetration depth) and the average vortex spacing a in the channel was chosen equal to that in the CE's, $a = a_0$.

For the periodic case, the CE potential is sinusoidal and the critical current density j_c is given by its maximum slope $j_c = \mu\Phi_0$. Simulating a chain of limited length was sufficient since all vortices behave as a single particle. Figure 2 shows an example of the ML step for superimposed rf-drive of amplitude $v_{ac}/(fa) = 2$ and frequency $f \simeq 3f_p$. In Fig. 2(c), we summarize the numerical results of $\Delta j_{max,P}$ versus frequency, represented by the solid squares. Here, $\Delta j_{max,P}$ is normalized by j_c and the frequency is normalized by f_p defined by Eq.(2.7). At high frequency $f > f_p$, $\Delta j_{max,P}$ saturates at a frequency independent value $\Delta j_{s,P}/j_c \simeq 1.13$ very close to the theoretical prediction Eq.(2.5) for periodic pinning. For smaller f, $\Delta j_{max,P}$ starts to decrease around f_p and then vanishes linearly with f. The whole frequency dependence of $\Delta j_{max,P}$ is well approximated by an empirical function

$$\Delta j_{max} = \Delta j_s \tanh(f/0.7f_p), \tag{2.9}$$

in which we have omitted the subscript referring to the periodic pinning potential. Equation(2.9) is represented by the solid line in Fig. 2(c).

For the *disordered* 1D channel, the CE vortices are assigned relatively large random shifts over distances $|\mathbf{d}|$ with $\sqrt{\langle(\nabla\cdot\mathbf{d})^2\rangle} = 0.12$ with respect to the regular lattice configuration [35,36]. We used a chain of 2000 vortices for which the results have become length-independent. Due to the disorder, both the numerically obtained threshold force $\propto j_c^R$ and the step width $\Delta j_{max,R}$ are strongly reduced (by a factor ~ 5, [35]) with respect to the ordered case. An example of the simulated ML step is shown in Fig. 2(b). There are two distinct differences with the periodic case, displayed in Fig. 2(a): (*i*) the sharp corners disappear and (*ii*) both below and above the ML condition the curve in (b) is essentially linear with the same slope, with a shift at the ML condition, very similar to the experimental result in Fig. 1(c). After normalization $\Delta j_{max,R}/j_c^R$ and $f/f_p = \gamma af/(j_c^R\Phi_0)$, we plot the simulation results collected for various frequencies in Fig. 2(c) as the open squares. The saturation value $\Delta j_{max,R}(f \gg f_p) \equiv \Delta j_{s,R} \simeq 0.7 j_c^R$, very close to the result in the random pinning limit in Eq.(2.6). The whole frequency dependence is then again well approximated by Eq.(2.9) (dashed line in Fig. 2(c)) in which we have now implicitly assumed the subscript 'R' referring to the quantities in the random case.

It is worth mentioning that the results for the disordered channel were insensitive to small changes in the ratio a/a_0. Further, we note that both in the periodic and the disordered channel simulations ML can be observed down to $f = 0$. We believe this is a direct consequence of the fact that vortices in the chain remain elastically connected, because other simulations in which also transverse degrees of freedom and plasticity are allowed, do not show this feature [37].

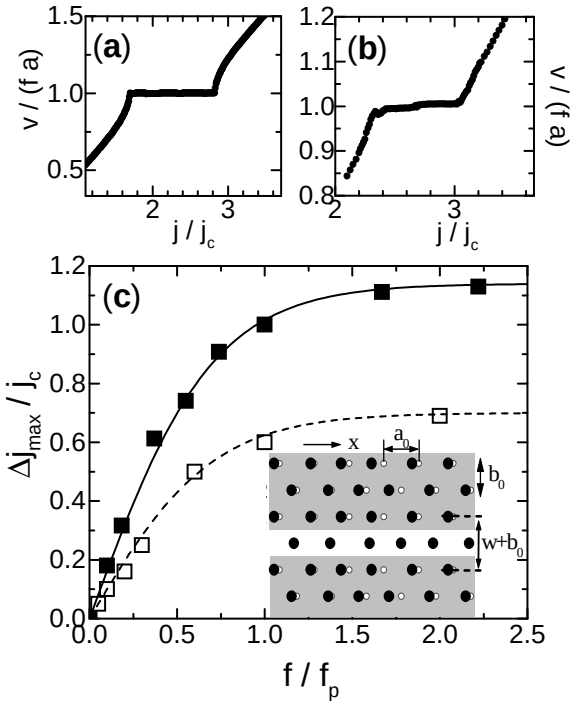

FIG. 2. (a) Normalized force-velocity curves for simulations of a vortex chain with an rf-drive of frequency $f = 3f_p$ and amplitude $v_{ac}/(fa) = 2$ in a periodic 1D-channel; (b) same as (a) in a disordered 1D channel. (c) Maximum ML current density step width from simulations with rf-drive of various frequencies and amplitudes: (■) results for a channel with periodic CE vortices; (□) results for disordered 1D channels. The curves show the empirical relation Eq.(2.9) with $C = 1.16$ (drawn line) and $C = 0.69$ (dashed line). The inset shows the simulation geometry for a periodic CE configuration (○) and for a disordered CE configuration (●).

III. EXPERIMENTAL

The device consists of a strong pinning layer of polycrystalline NbN film on top of a weak pinning amorphous (a-) $Nb_{1-x}Ge_x$ film ($x \approx 0.3$). The thickness of the NbN and a-NbGe films are 50 and 550nm, respectively. Using reactive ion etching with proper masking [38], narrow straight channels were etched from the top (NbN) layer leaving a 300nm(=d_{ch}) thick (a-NbGe) bottom layer, see Fig. 1(a). The width and length of each channel are 230nm and 300μm(= L), respectively. The spacing between adjacent channels is 10 μm. Magnetic field was applied perpendicular to the films, inducing a vortex array as schematically shown in Fig. 1(b). The transport current was applied perpendicularly to the channel, providing a driving force parallel to the channel.

For the ML measurement, we recorded dc voltage by

sweeping the dc current with superimposed rf-current. The transmission lines for the rf-current were terminated by matching circuits very close to the sample. To avoid heating, both the sample and the circuits were immersed in superfluid ^{4}He. For consistency, all the data presented in this paper were taken after field cooling in which the magnetic field was applied above T_c's of a-NbGe (2.68K) and NbN(11K) and the sample subsequently cooled to T =1.9K, which is much lower than the vortex lattice melting temperature $\approx 2.5K$ for the fields we studied. The ML steps in IV curves are always rounded like in Fig. 1(c). For definition of the current step width ΔI, we took the derivative of the IV curve and integrated over the ML peak in the differential conductance-voltage curve with respect to the flux-flow base line [21].

IV. RESULTS

Our measurements were carried out in the magnetic field regime where 3-chain structures exist in the channels, ranging from 45 to 110mT, see Fig. 1(d). We thus focus on the fundamental ML step characterized by $V_{1,1}/(\Phi_0 f N_{ch}) = 3$ originating from *coherently moving* $n = 3$ regions. At the borders of our field range coexistence with $n = 2$ or $n = 4$ ML steps may occur.

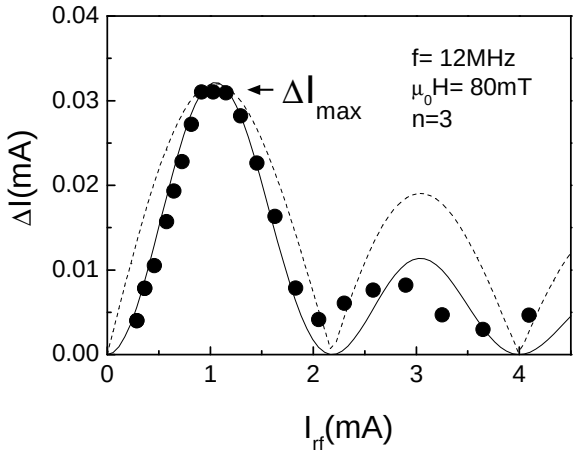

FIG. 3. Current width ΔI of the fundamental ML step vs. rf current I_{rf} taken at 12MHz and 80mT. The maximum value ΔI_{max} is indicated. Solid and dotted curves display $\Delta I \propto J_1^2(z)$ and $\Delta I \propto |J_1(z)|$, with $z \propto I_{rf}$, respectively.

In Fig. 3 we show an example of how the fundamental ML width ΔI depends on the rf drive I_{rf} for $\mu_0 H$ = 80mT and f = 12MHz. $\Delta I(I_{rf})$ shows oscillatory behavior with a maximum value ΔI_{max} in the first lobe, as indicated in the figure. A qualitative comparison of the data with the theoretical predictions Eq.(2.3) (solid line) and Eq.(2.2) (dotted line) shows that the data follows more closely a J_1^2 than a $|J_1|$ dependence. At ΔI_{max} it is found that $I_{rf} = (1.9\pm0.3)I_{dc}$ over a broad frequency range between f_p and 40 MHz (above this frequency the experimental error in I_{rf} becomes larger). This value is in good agreement with Eq.(2.3) which has a maximum at $z = v_{ac}/fa = v_{ac}/v_{dc} \approx I_{rf}/I_{dc} = 1.8$. It is important to note that while the values of the rf-current might appear rather large, the actual vortex displacements due to the rf-drive at or below the first maximum in $J_1^2(z)$, are less than $1.8/(2\pi) \simeq 0.3$ of the lattice spacing.

The $J_1^2(z)$ behavior shows that the pinning potential due to the vortices in the CE acts as a random potential (RP) [39]. The origin of the RP is the strong positional disorder of the vortex lattice in the NbN edge material. This disorder has recently been observed in scanning tunnelling microscopy experiments on NbN films [40]. We further note that we did not observe subharmonic ML steps, i.e. there were no ML steps at $V_{ML} = 3f\Phi_0 N_{ch}/q$ with $q \geq 2$. In the context of our RP this seems in contradiction to the results of others [18]. But those experiments have been carried out at relatively low fields where the RP has short range correlations on a scale $\xi \ll a$. Fourier components qk with $q \geq 2$ are needed to describe such short range fluctuations and therefore subharmonic ML steps are seen. In our case, the RP is due to the CE vortices which have average spacing $a_0 \simeq a$. Consequently the most important Fourier component describing this RP is the $q = 1$ mode, which explains why we do not see subharmonic ML steps.

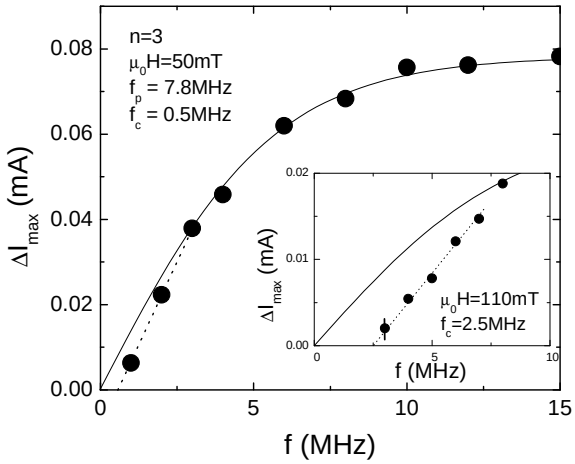

FIG. 4. The maximum current width ΔI_{max} as a function of frequency f at 50mT. The solid curve shows the fit according to the empirical function Eq.(2.9). The dotted line shows the linear extrapolation to $\Delta I_{max} = 0$ for definition of the dynamic ordering frequency f_c. The inset shows the onset behavior of ΔI_{max} and ordering frequency f_c for a field of 110mT. The solid curve shows a fit of the high frequency data to Eq.(2.9).

Next we turn to the frequency dependence of ΔI_{max}. Figure 4 shows $\Delta I_{max}(f)$ at 50 mT obtained from measurements similar to those in Fig. 3 at various frequencies. As in the numerical results in Fig. 2(c), ΔI_{max} saturates at a value $\Delta I_s \simeq 78$ μA at high frequencies, while at low frequencies it decreases monotonically with f. A large part of the data is well approximated by the empirical function discussed in the previous section,

$\Delta I_{max} = \Delta I_s \tanh(f/0.7f_p)$, and we can extract the pinning frequency f_p=7.8MHz as the remaining fit parameter. However, at low frequency (i.e. small dc-velocity) the data lie significantly below the empirical curve. This implies that the vortex motion becomes less coherent due to the disordered CE's. On reducing f, ΔI_{max} vanishes almost linearly at a *finite* frequency f_c determined by the intersection between the dotted line and the $\Delta I_{max} = 0$ axis. In this regime, the rf-current for which ΔI exhibits its maximum value, starts to saturate at a value $\sim I_c$ [41]. The collapse of ΔI_{max} at finite frequency f_c is even more clearly visible in the data taken at 110mT shown in the inset to Fig. 4. Below f_c no ML step appears at *any rf drive*, indicating the complete absence of coherent 3-row motion.

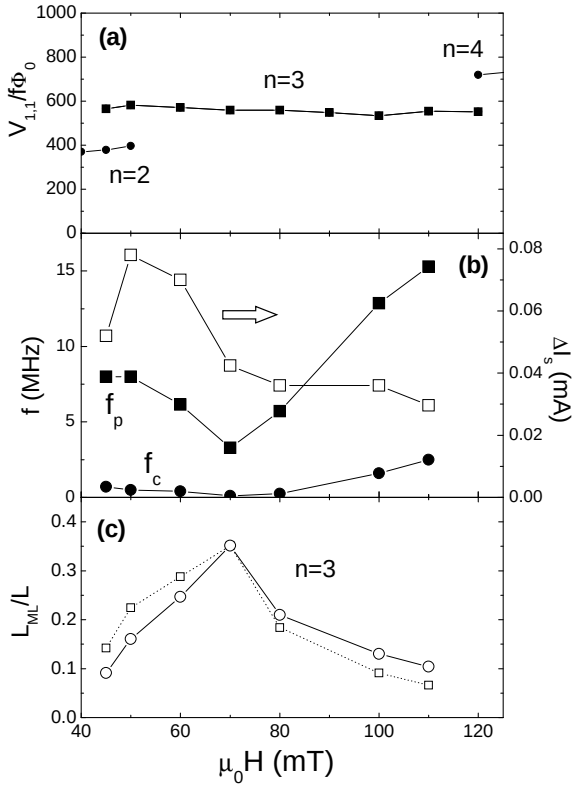

FIG. 5. (a) $V_{1,1}/f\Phi_0$ versus field. (b) The pinning frequency f_p (■), the dynamic ordering frequency f_c (•), and the saturation value of the maximum current width ΔI_s (□) for $n = 3$ as a function of field. The data are obtained from fits to the measured $\Delta I_{max}(f)$. (c) The coherently moving fraction L_{ML}/L of $n = 3$ regions vs. field, where L_{ML} is determined from Eq.(4.1), with $a = a_0(B)$ (□) and $a = a_M B_M/B$ (○), where the subscript 'M' refers to the matching field, see text. All lines are guides to the eye.

The above fitting analysis was performed on $\Delta I_{max}(f)$ data taken at various fields in the $n = 3$ field regime and we extracted f_p, ΔI_s and the dynamic ordering frequency f_c. We first discuss the results of f_p and ΔI_s as a function of magnetic field, shown in Fig. 5(b). As observed, f_p has a minimum at 70 mT, somewhat below the middle of the plateau in $V_{1,1}$ in Fig. 5(a), and it increases on approaching either end of the plateau. Hence, the associated pinning current density in the coherent 3-chain regions $\tilde{j}_c(k)$ is small at 70 mT and increases away from 70 mT. In fact, the value of $\tilde{j}_c(k)$ as determined from f_p using Eq.(2.8) agrees within 30% with j_c as determined directly from dc-IV curves, Fig. 1(e). Meanwhile, ΔI_s exhibits a field dependence which differs considerably from that of f_p: it has a broad peak around $B = 50$ mT and then decreases with increasing field. Clearly, this behavior can not be explained by simply assuming $\Delta I_s(B) \propto j_c(B) \propto f_p(B)$.

At this point we note that theory assumes all vortices in the channel are moving coherently. However, in our experiment only a fraction of the vortices move coherently. Specifically, an n-row region may locally break up due to the strong edge disorder or it may coexists with $n \pm 1$-row regions (with different ML voltages) due to mismatch [21]. We define the total length of mode-locked regions with 3 coherently moving rows as L_{ML} and the mode-locked fraction as L_{ML}/L. Since only the coherent n-row regions contribute to ΔI_s, we can link the value of ΔI_s to that of Δj_s by using $\Delta I_s = L_{ML} d_{ch} \Delta j_s$. In this expression Δj_s can be obtained from the measured pinning frequency via Eq.(2.8) and (2.6). Using $\gamma = \Phi_0 B/\rho_f$ the result for L_{ML} is given by

$$L_{ML} = \frac{\Delta I_s}{f_p a} \frac{\rho_f}{0.67 B d_{ch}} \tag{4.1}$$

The different field dependencies of ΔI_s and f_p mentioned above should thus be attributed to an additional field dependence of L_{ML}.

We now evaluate L_{ML} using ρ_f for amorphous NbGe films [42,43] and first assume an equilibrium lattice spacing $a = a_0 (\simeq 1.075\sqrt{\Phi_0/B})$ with $B = \mu_0 H$. Figure 2(c) shows L_{ML} normalized by the channel length L vs. field (square symbols). As observed, the coherently moving fraction is maximum at $B \simeq 70$ mT. This provides a clear definition of the matching field B_M for $n = 3$. At B_M, the longitudinal spacing a in the channel should obey $a \equiv a_M = a_0$ and the row spacing $b_M = \Phi_0/B_M a_M$ is commensurate with the effective channel width, i.e. $3b_M = w$. However, away from the matching field the array will be frustrated (stretched or compressed) due to the confinement. In particular, for $B < B_M$ the lattice spacing $a > a_0$, while for $B > B_M$, $a < a_0$. The maximum possible difference between a and a_0 would be achieved when the row spacing b would not change with mismatch, i.e. $b(B) = b_M$ [44]. This would imply $a = (B_M/B)a_M$. Inserting this relation for a in Eq.(4.1), the result for L_{ML}, shown by the open circles, is slightly modified but shows essentially the same behavior as our first analysis: upon increasing the frustration, which we define as $|1-(B/B_M)|$, the spatial extent of regions with 3 coherently moving rows shrinks progressively. An additional analysis of the $n = 2$ ML steps which occur at lower fields ($B \simeq 50$mT, where the transition $n = 3 \rightarrow 2$ takes place), shows consistently that the spatial extent of

the 2 row ML regions increases upon further decreasing field.

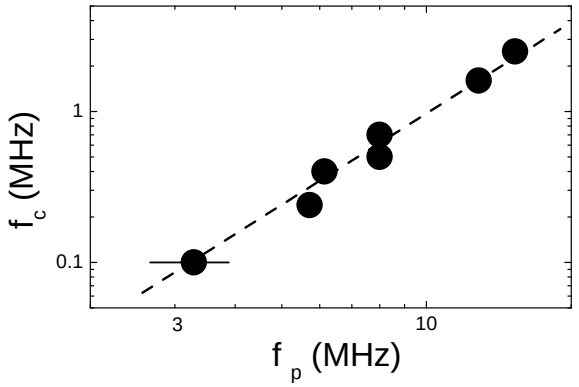

FIG. 6. Dynamic ordering frequency f_c versus pinning frequency f_p. Dotted line: $f_c = \tau f_p^2$ with $\tau \simeq 1 \cdot 10^{-8}$ s.

Finally we discuss the behavior of the ordering frequency f_c. As shown in Fig. 5(b), $f_c(B)$, denoted by (•), exhibits a minimum at the matching field and systematically increases with mismatch. Similarly to the decay of L_{ML} with increasing frustration, this shows that a larger mismatch progressively induces more disorder. We also find that, when the field is reduced below $B \simeq 50$ mT, where a 2-row configuration first appears, the ordering frequency $f_c^{n=2}$ for the emergence of the $n = 2$ ML effect decreases.

Qualitatively, the behavior of f_c is similar to that of the pinning frequency f_p (or I_c). Both are important quantities characterizing the random pinning of a system and are not independent, as follows from a double logarithmic plot of f_c as a function of f_p, shown in Fig. 6. The data are well described by the relation $f_c = \tau f_p^2$ with $\tau \simeq 1 \cdot 10^{-8}$ s, represented by the dashed line. A more detailed fit of the data using a power law relation $f_c \propto f_p^{\alpha}$ yields an exponent $\alpha = 2.1 \pm 0.1$.

V. ANALYSIS AND DISCUSSION OF DYNAMIC ORDERING AND DEPINNING THRESHOLD BEHAVIOR

A. Comparison with the KV theory

For a proper discussion of the above results, we first shortly describe the phenomenological ordering theory of Koshelev and Vinokur (KV) [1]. In their study of a 2D vortex system with strong random bulk pinning, they found that the shaking action due to motion through the pinning potential can be represented by a 'shaking temperature' T_{sh} which decreases with velocity as $T_{sh} \propto 1/v$. The dynamic ordering transition occurs when the effective temperature $T+T_{sh}$ is reduced below the equilibrium melting temperature T_m, i.e. when the velocity exceeds $v_c \propto 1/(T_m - T)$. In later work [4,45] it was shown that the shaking temperature refers to (bond) fluctuations transverse to the velocity and that the associated ordering at v_c corresponds to so called transverse freezing, where inter-chain excursions (permeation modes) are strongly suppressed. Within the KV theory we can express the ordering frequency $f_c = v_c/a$ as:

$$f_c = \sqrt{3/2\pi}\frac{\gamma_u \rho_f}{\Phi_0^2 a^2 d_{ch} k_B (T_m - T)}, \tag{5.1}$$

with γ_u the mean squared $2D$ pinning energy multiplied by the area of a pin, ρ_f the flux flow resistivity, a the lattice spacing and d_{ch} the film thickness.

In our channel system the ordering can also be described as transverse freezing. We observed this in simulations (e.g. for $w/b_0 \simeq 3$) as a suppression of the inter-chain excursions in parts of the channel at sufficient velocity [37]. However, different from the 2D system considered by KV, these inter-chain excursions and the associated shaking temperature now arise from the random interaction with the disordered vortices in the CE's and a modification of Eq.(5.1) is required. Thinking in terms of bond fluctuations or a Lindemann criterion, as in [4], it is clear that it is the short wavelength $\sim a_0$ disorder component in the potential due to quenched vortex displacements $\mathbf{d}$ in the CE which is relevant for the 'shaking temperature'. This component acts only in a range $\sim a_0/2$ from the first pinned row [37], therefore shaking of the outer rows should govern the transverse freezing. A rough estimate within London theory yields an rms-amplitude of the random stress near the edge $\sim \varepsilon_{ce} c_{66}$ with c_{66} the shear modulus and $\varepsilon_{ce} \simeq (\sqrt{\langle |\mathbf{d}|^2 \rangle}/a_0)/(\pi\sqrt{3})$ representing the random strain [16,37]. Taking the longitudinal range of a pin also to be $a_0/2$, we replace the parameter γ_u in Eq.(5.1) by γ_{ce}, resulting in:

$$\gamma_{ce} \simeq (\varepsilon_{ce} c_{66} a_0 b_0 d_{ch})^2 (\frac{a_0}{2})^2. \tag{5.2}$$

Further it is important to realize the following: the energy scale $k_B T_m$ in Eq.(5.1) should be regarded as the energy for creation of the dislocation pairs that are required for plastic motion i.e. $k_B T_m \rightarrow k_B T_p \simeq c_{66} a_0^2 d_{ch}/(2\pi)$, with c_{66} evaluated at the field and temperature of the measurement [46]. For our temperature and fields, this energy $k_B T_p$ is two orders of magnitude larger than the thermal energy $k_B T$ which we can therefore neglect in Eq.(5.1). Hence, the random shaking ($\propto 1/v$) in our case essentially represents 'cold working' of the moving structure. We also anticipate that the energy $k_B T_p$ should depend on the matching condition since a reduction of this energy eventually drives the transition to $n = 2$ or $n = 4$ rows. Therefore we add a mismatch dependent factor A_p: $k_B T_p = A_p c_{66} a_0^2 d_{ch}/(2\pi)$, where A_p is assumed to be 1 at matching. Taking into account these changes, Eq.(5.1) becomes

$$f_c \simeq \frac{\sqrt{\pi}\varepsilon_{ce}^2 c_{66} \rho_f}{2 A_p \Phi_0 B} \tag{5.3}$$

Using the experimental parameters with $c_{66} = \Phi_0 B/(16\pi\mu_0\lambda^2)$ and $\lambda(1.9\ \mathrm{K}) \simeq 1.1\ \mu$m, we obtain the value of ε_{ce} from the value of f_c at matching: $\varepsilon_{ce} \simeq 0.025$, i.e. $\sqrt{\langle|\mathbf{d}|^2\rangle}/a_0 \simeq 0.13$. This is in very reasonable agreement with our estimate ($\sqrt{\langle|\mathbf{d}|^2\rangle}/a_0 \simeq 0.10$) near the melting temperature in [16]. From Eq.(5.3) and the f_c data in Fig. 5(b) we can also extract the field dependence of A_p characterizing the reduction of the defect creation energy. The result is plotted in Fig. 7, showing that close to mismatch A_p has decreased by an order of magnitude.

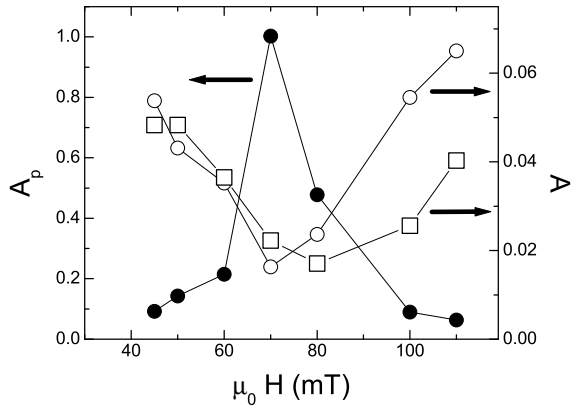

FIG. 7. (•) The parameter A_p as determined from f_c in Fig. 5(b) and Eq.(5.3) using $\varepsilon_{ce} = 0.025$. (□) The parameter A describing the pinning strength determined directly from Eq.(5.4) and the measured critical current density. (○) A determined from Eq.(5.5) using the field dependence of A_p and $\tau = 10^{-8}$ s.

Next, we turn to the relation between f_c and f_p. The dc-critical current density can be described phenomenologically by [25]:

$$j_c = 2Ac_{66}/(Bw), \tag{5.4}$$

where in our case A varies from $A \simeq 0.015$ at matching to $A \simeq 0.04 - 0.05$ at mismatch, see the open squares in Fig. 7. Further, when we combine Eqs.(5.1), (5.2), Eq.(5.4) with Eq.(2.8) and use $\gamma = \Phi_0 B/\rho_f$, we obtain the quadratic relation $f_c = v_c/a = \tau f_p^2$ observed experimentally in Fig. 6 with the timescale τ given by:

$$\tau \simeq 0.5(\varepsilon_{ce}/A)^2 \frac{(wB)^2}{A_p c_{66}\rho_f}. \tag{5.5}$$

Since $\rho_f, c_{66} \propto B$ and experimentally we found that $\tau \simeq 10^{-8}$ s, independent of field, this implies that $A \propto \sqrt{1/(\tau A_p)}$. Using this relation with the field dependent value of A_p, we obtain A as shown by the open circles in Fig. 7. The minima in both data are slightly shifted and deviations are seen for $B > B_m$, but given the approximations made, the overall agreement is still reasonable. An important physical implication of the relation $A \propto \sqrt{1/(A_p)}$ is that the increase in pinning strength away from matching is directly related to the reduction of the defect creation energy. In other words, the rise in A reflects an effective *softening* of the array in the channel upon increasing mismatch. Through this softening it is able to better adjust to the random CE pinning potential, very much analogous to the mechanism responsible for the peak-effect in ordinary superconductors [47]. In our case a more detailed picture of the softening mechanism is possible. We already mentioned that for $B > B_M$, the chains are longitudinally compressed ($a < a_0$). This will facilitate deviations in the transverse direction and reduce the energy to (dynamically) create interstitials between rows. For $B < B_M$, the chains are stretched, i.e. $a > a_0$. In this case the energy for a chain to accept vortices from a neighboring chain is lowered. This in turn facilitates a configurational change in which the array can better adopt to the CE potential. An additional mechanism for the rise in A for $B < B_m$ is that, due to the mismatch, the outer chains will be pushed towards the CE, leading to an enhanced influence of the CE potential.

To conclude this section, we want to mention that the relation $f_c \propto f_p^2$ is not specific to our channels, but can be obtained as a general result from the KV theory in the strong pinning limit.

B. dc versus dc+rf driven state

So far we have tacitly assumed that the flow behavior obtained from our rf-dc measurements simply reflects that of the dc-driven structure. We now discuss to what extent the additional rf-current itself influences the behavior. Recent measurements of the rf-impedance [48], which is a sensitive probe of ML at small rf-currents, have shown that on approaching the dc-driven state, i.e. when $I_{rf} \to 0$, the voltage broadening $\delta V_{1,1}$ of the fundamental ML step diverges. Since $\delta V_{1,1} \propto \delta f_{int}$, this broadening reflects fluctuations in the washboard frequency and, via $f = v/a$, fluctuations in the velocity and in the longitudinal lattice spacing a [49]. Correspondingly, the divergence of $\delta V_{1,1}$ implies that the dc-driven state lacks temporal coherence. We also did not observe any narrow band noise in the voltage spectrum of the dc-driven state (even for only 30 channels at large dc-drive). At the same time, $V_{1,1} \propto n$ remains constant for $I_{rf} \to 0$, from which we conclude that the dc-state still exhibits local regions organized in 3 moving chains. Thus, at sufficient velocity the dc-state would correspond to temporally incoherent, confined smectic regions [3] of finite (mismatch dependent) length, with liquid-like intra chain order and residual inter-chain excursions.

In presence of rf-current the fluctuations are strongly reduced, as also observed in experiments on CDW's [50]. In simulations we observed that the suppression of the inter-chain excursions plays an important role in this process, causing *transversely frozen* regions in the channel. However, the rf-dc IV curves always show incomplete ML with the same broadening $\delta V_{1,1}$ as discussed above.

This broadening is too large to be explained by the elastic theory in [26]. Therefore, it is either caused by residual slip in the n-row regions or by remaining plastic regions with interconnecting rows, but further experimental and numerical work is required to decide on this issue.

Finally, we shortly return to the frequency dependence of the ML current width ΔI_{max} in Fig. 4. Extending the relation $\Delta I_{max}(f) \propto \Delta j_{max}(f) L_{ML}(f)$ to frequencies below f_p and taking the ideal $\tanh(f)$ behavior Eq.(2.9) for Δj_{max}, we find that the ordering frequency f_c would mark the velocity where $L_{ML} \to 0$. Such interpretation implies that the dynamic ordering in our disordered system is a smooth, second order dynamic phase transition.

VI. SUMMARY

Using mode-locking experiments, we have investigated the dynamics of vortex arrays confined in disordered mesoscopic channels. The ML effect allows to trace in detail structural transitions from $n-1 \to n \to n+1$ confined moving vortex chains on changing field. A study of the amplitude and frequency dependence of the ML steps and comparison to simulations of an *elastic* chain provide a complete characterization of the pinning strength, dynamic ordering velocity and coherency of the arrays. We find that the spatial extent L_{ML} of coherently moving n row regions is large at a matching field and shrinks with increasing mismatch. At the same time both the pinning frequency $f_p \propto j_c$ and the ordering frequency f_c (proportional to the ordering velocity) increase with mismatch. We show that $f_c \propto f_p^2$. Together with our previous observation of a divergence of f_c near the melting temperature in [16], these results provide detailed experimental evidence for the phenomenological ordering theory of Koshelev and Vinokur [1].

VII. ACKNOWLEDGEMENTS

We like to thank A. Koshelev for stimulating discussion. This work was supported by the 'Stiching voor Fundamenteel Onderzoek der Materie' (FOM) and the ESF-Vortex program.

[1] A.E. Koshelev and V.M. Vinokur, Phys. Rev. Lett. **73**, 3580 (1994).

[2] T. Giamarchi and P. Le Doussal, Phys. Rev. Lett. **76**, 3408 (1996); P. Le Doussal and T. Giamarchi, Phys. Rev. B **57**, 11356 (1998).

[3] L. Balents, M.C. Marchetti and L. Radzihovsky, Phys. Rev. B **57**, 7705 (1998); L. Balents and M.P.A. Fisher Phys. Rev. Lett. **75**, 4270 (1995).

[4] S. Scheidl and V.M. Vinokur, Phys. Rev. B **57**, 13800 (1998); Phys. Rev. E **57**, 2574 (1998).

[5] M.C. Faleski, M.C. Marchetti, and A.A. Middleton, Phys. Rev. B **54**, 12427 (1996).

[6] K. Moon, R.T. Scalettar and G.T. Zimanyi, Phys. Rev. Lett. **77**, 2778 (1996); S. Spencer and H.J. Jensen, Phys. Rev. B **55**, 8473 (1997); A.B. Kolton, D. Dominguez and N. Grønbech-Jensen, Phys. Rev. Lett. **83**, 3061 (1999).

[7] A.B. Kolton and D. Dominguez, N. Grønbech-Jensen, Phys. Rev. Lett. 86, 4112 (2001).

[8] M. Marchevsky, J. Aarts, P.H. Kes, M.V. Indenbom, Phys. Rev. Lett. **78**, 531 (1997).

[9] F. Pardo, F. de la Cruz, P.L. Gammel, E. Bucher, and D.J. Bishop, Nature **396**, 348 (1998).

[10] A.M. Troyanovski, J. Aarts and P.H. Kes, Nature **399**, 665 (1999).

[11] S. Bhattacharya and M.J. Higgins, Phys. Rev. Lett.**70**, 2617 (1993).

[12] M.C. Hellerqvist, D. Ephron, W.R. White, M.R.Beasley, and A. Kapitulnik, Phys. Rev. Lett. **76**, 4022 (1996); M.C. Hellerqvist, and A. Kapitulnik, Phys. Rev. B **56**, 5521 (1997).

[13] J.M.E. Geers, C. Attanasio, M.B.S. Hesselberth, J. Aarts, and P.H. Kes, Phys. Rev. B 63, 094511 (2001).

[14] Y. Paltiel, Y. Myasoedov, E. Zeldov, G. Jung, M.L. Rappaport, D.E. Feldman, M. J. Higgins and S. Bhattacharya, Phys. Rev. B 66, 060503 (2002).

[15] K.E. Bassler, M. Paczuski, and E. Altshuler, Phys. Rev. B **64**, 224517 (2001).

[16] R. Besseling, N. Kokubo and P.H. Kes, cond-mat/0302187.

[17] Y. Togawa, R. Abiru, K. Iwaya, H. Kitano and A. Maeda, Phys. Rev. Lett. **85**, 3716 (2000).

[18] A.T. Fiory, Phys. Rev. Lett. **27**, 501 (1971); Phys. Rev. B **7**, 1881 (1973); Phys. Rev. B **8**, 5039 (1973); J.M. Harris, N.P. Ong, R. Gagnon, and L. Taillefer, Phys. Rev. Lett. **74**, 3684 (1995); Y. Togawa, H. Kitano, and A. Maeda, Physica C **378**, 448 (2002).

[19] P. Martinoli, O. Daldini, C. Leemann and E. Stocker, Solid State Comm. **17**, 205 (1975).

[20] L. Van Look, E. Rosseel, M.J. Van Bael, K. Temst, V.V. Moshchalkov, and Y. Bruynseraede, Phys. Rev. B **60**, R6998 (1999).

[21] N. Kokubo, R. Besseling, V.M. Vinokur, and P.H. Kes, Phys. Rev. Lett. **88**, 247004 (2002).

[22] G. Grüner, Rev. Mod. Phys. **60**, 1129 (1988).

[23] R.E. Thorne, W.G. Lyons, J.W. Lyding, J.R. Tucker, and J. Bardeen, Phys. Rev. B **35**, 6360 (1987).

[24] Ch. Leeman, Ph. Lerch, and P. Martinoli, Physica B **126**, 475 (1984); S.P. Benz, M.S. Rzchowski, M. Tinkham, and C.J. Lobb, Phys. Rev. Lett. **64**, 693 (1990); K. Ravindran, L.B. Gomez, R.R. Li, S.T. Herbert, P. Lukens, Y. Jun, S. Elhamri, R.S. Newrock, and D.B. Mast, Phys. Rev. B **53**, 5141 (1996).

[25] A. Pruymboom, P.H. Kes, E. van der Drift and S. Radelaar, Phys. Rev. Lett. **60**, 1430 (1988); M.H. Theunissen, E. Van der Drift, and P.H. Kes, *ibid.* **77**, 159 (1996).

[26] A. Schmid and W. Hauger, J. Low. Temp. Phys. **11**, 667 (1973).

[27] A.I. Larkin and Yu.N. Ovchinikov, Sov. Phys. JETP, **38**,

854 (1974).
[28] P. Martinoli, Phys. Rev. B **17**, 1175 (1978).
[29] M. Tinkham, *Introduction to Superconductivity* (McGraw-Hill International Editions, 1996).
[30] For convenience we use the same symbol f_p both for the periodic and the random pinning cases. In the following it will be clear from the context which one we use.
[31] For sinusoidal pinning, $\Delta j(f \ll f_p)$ can be obtained analytically for small rf-amplitude $j_{rf} \ll j_c$, see M.J. Renne and D. Polder, Rev. de Phys. Appliquee, **9**, 25 (1974). However, both our simulations and those in [32] show that the maximum value $\Delta j_{max}(f \ll f_p)$ is achieved for $j_{rf} \simeq j_c$, for which the analytical approach fails.
[32] P. Russer, J. Appl. Phys. **43**, 2008 (1972).
[33] M. Octavio, J.U. Free, S.P. Benz, R.S. Newrock and D.B. Mast, and C.J. Lobb, Phys. Rev. B **44**, 4601 (1991).
[34] R. Besseling, R. Niggebrugge and P.H. Kes, Phys. Rev. Lett. **82**, 3144 (1999).
[35] R. Besseling, T. Dröse, V.M. Vinokur and P.H. Kes, Europhys. Lett. **62**, 419 (2003).
[36] R. Besseling, Ph. D. Thesis, Leiden University (2001).
[37] R. Besseling *et al.*, in preparation.
[38] E. van der Drift, S. Radelaar, A. Pruymboom, P.H. Kes, J. Vac. Sci. Technol. **B6**(1), 297 (1988).
[39] In recent measurements on 'bulk' NbGe films where pinning originates from intrinsic disorder in the film, $\Delta I(I_{rf})$ exhibited an even closer correspondence to the relation $\Delta I(I_{rf}) \propto J_1^2(z)$ at high frequency, see R. Besseling, O. Benningshof, N. Kokubo, and P.H. Kes, to be published, cond-mat/0304046.
[40] G.J.C. van Baarle, A.M. Troianovski, T. Nishizaki, P.H. Kes, and J. Aarts, Appl. Phys. Lett. **82**, 1081 (2003).
[41] In the 1D simulations (both for ordered and disordered channels) a similar saturation of the 'optimum' rf-current was observed for the ML steps with $f \downarrow 0$, see also [31,32].
[42] P. Berghuis and P.H. Kes, Phys. Rev. B **47**, 262 (1993).
[43] A.I. Larkin and Yu. Ovchinikov, J. Low Temp. Phys. **34**, 409 (1979);
[44] In reality the row spacing b away from a matching field will be in between b_M and b_0. Therefore the true behavior of L_{ML}/L will lie between the dashed and the full curve in Fig. 5(c).
[45] A.B. Kolton, R. Exartier, L.F. Cugliandolo, D. Dominguez, and N. Grønbech-Jensen, Phys. Rev. Lett. **89**, 227001 (2002).
[46] V.M. Vinokur, P.H. Kes, and A.E. Koshelev, Physica C **168**, 29 (1990).
[47] A.B. Pippard, Phil. Mag. **19**, 217 (1969).
[48] N. Kokubo, R. Besseling and P.H. Kes, Physica C, to be published.
[49] We note that $\delta V_{1,1}$ is much too large to be attributed to a spread in j_c from channel to channel, which was further confirmed by measurements on only 30 channels.
[50] For CDW's, (broadened) narrow band noise is generally present in the dc-case. Additional rf-driving leads to further synchronization at mode-locking, as shown in S. Bhattacharya, J.P. Stokes, M.J. Higgins, and R.A. Klemm, Phys. Rev. Lett. **59**, 1849 (1987). This is consistent with a diverging velocity correlation length at ML, as shown by H. Matsukawa, J. Ph. Soc. Jap. **56**, 1522 (1987); *ibid.* **56**, 1507 (1987).